IEEE Control Systems Letters paper presented at
2023 American Control Conference (ACC)
San Diego, CA, USA. May 31 - June 2, 2023

State and Parameter Estimation for Stochastic Open Two-Level Quantum Systems

Emilio Corcione[1] and Cristina Tarin
Institute for System Dynamics & Research Center SCoPE, University of Stuttgart, 70563 Stuttgart, Germany

***Abstract*— Research in the field of quantum control usually assumes complete knowledge of the state and parameters. In this paper, a driven and damped two-level quantum system under continuous observation is considered. Its time evolution is governed by an operator-valued stochastic master equation and conditioned on the recorded measurement data. The system is transformed to state space representation and its observability is proven analytically. An extended Kalman filter is employed in order to both reconstruct the density operator describing the full state of the system, and to dynamically identify key parameters. Convincing results are obtained in numerical simulations. Overall, a practical engineering approach to quantum control is presented.**

I. INTRODUCTION

In recent years, with the emergence of next generation quantum technologies, the gap between quantum mechanics and classical engineering has been bridged. Of particular interest for both fundamental research and development is the adaptation of system theoretical approaches and control engineering methods. Controlling a system implies stabilising and driving it to a desired state in the presence of uncertainties and disturbances. Using continuous measurements of the system thereby significantly improves the control performance. Due to the unusual nature of quantum mechanical systems, transferring and implementing classical control techniques is not straightforward, but presents an interesting challenge [1], [2].

Most literature on the control of systems with quantum mechanical properties either considers only Schrödinger pure state dynamics [3], [4] or assumes full knowledge of both the state of the system as well as all its parameters [5], [6]. Approaches to make quantum control more practically feasible were presented in [7] and [8], where imperfect detection and feedback delay were taken into account, respectively. First steps towards dynamical parameter estimation based on Bayesian statistics were reported by [9] and further developed by [10], [11]. In particular, the information gain concerning the unknown Rabi frequency driving a two-level atom is investigated. A parameter identification scheme based on the analytically derived equilibrium point of an open two-level quantum system is presented in [12]. Here, the decoherence rate is estimated from continuous measurements, however, the implementation of the proposed feedback control law requires further parameter values.
Dynamical quantum state estimation based on least-squares minimisation and compressed sensing is explored by [13] and extended to include a state transfer feedback control by [14]. Moreover, to reconstruct the quantum state associated with the total spin of alkali atoms, Bayesian filtering techniques have successfully been adapted [15], [16]. For this, the stochastic backaction of the quantum measurement process on the system has been neglected. In [17], the analytical proof is provided, that when using an appropriate feedback control and having full knowledge of all relevant parameters, the state of a continuously monitored spin-$\frac{1}{2}$ system can be reproduced by exploiting the direct coupling between the system dynamics and the measurement record. In [18], [19], the theoretical applicability of an analogue of the classical Kalman filter for state estimation in linear quantum systems is derived. However, their analysis is restricted to (quasi-classical) Gaussian states. A Kalman filter has also been used by [20], [21] in atomic magnetometry to estimate the spin component in z-direction as well as the strength of an external magnetic field, but only a simplified and heavily reduced system is considered.

To the authors' best knowledge, at the time of writing, no conventional observer for state and parameter estimation has been properly proposed, and research in quantum control is mostly theory driven. Within the scope of this paper, we aim to step away from theory and towards a more engineering related approach to quantum control: Our main contribution is the application of a classical method of control engineering to quantum mechanics. Specifically, a Kalman filter is employed to both estimate the full state of a quantum system and to dynamically identify key parameters at the same time. Thereby, a practical framework for further research in the field of quantum control is established.

II. SYSTEM MODEL

Widely considered the simplest quantum system of relevance, the two-level system exhibits several system theoretically interesting quantum characteristics and has successfully been used to model e.g. atoms interacting with light, spin-$\frac{1}{2}$ systems like electrons or qubits, the building blocks for modern quantum technologies [22]. In any case, apart from the parameters, the mathematical structure of the system remains the same. Moreover, the transition to N-level systems is mostly straightforward, which further increases its theoretical significance. As this paper aims to provide a proof of concept regarding the application of a core method of control engineering to quantum mechanics, we won't consider any specific physical system, but rather a generic open two-level

[1]Correspondence: emilio.corcione@isys.uni-stuttgart.de

system. In this section, a suitable mathematical model is derived in Dirac notation.

In Fig. 1, a schematic abstraction of a driven and damped two-level system is shown. As the name suggests, only two

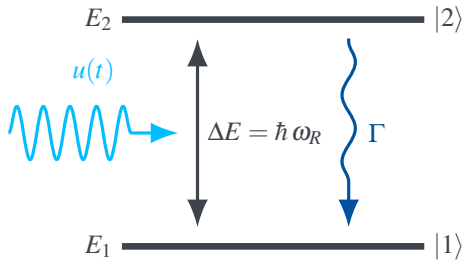

Fig. 1. Schematic representation of a damped and driven two-level quantum system.

discrete energy levels E_1 and $E_2 > E_1$ are considered here. These are associated to the energy eigenstates $|1\rangle$ and $|2\rangle$, which form an orthonormal basis of the two-dimensional complex Hilbert space $\mathbb{C}^2$ of pure system states. Visualised by the dark blue snake arrow, the system is damped, i.e. it decays from the energetically excited state $|2\rangle$ to the ground state $|1\rangle$ by rate $\Gamma > 0$. Level transitions are described using the non-Hermitian raising and lowering operators

$$\begin{aligned} \sigma_+ &= |2\rangle\langle 1|, \\ \sigma_- &= |1\rangle\langle 2| = \sigma_+^\dagger. \end{aligned} \tag{1}$$

These result from the eigenproblem

$$\begin{aligned} \sigma_+|1\rangle &= |2\rangle & \sigma_-|1\rangle &= 0 \\ \sigma_+|2\rangle &= 0 & \sigma_-|2\rangle &= |1\rangle \end{aligned}$$

and allow to define the three Hermitian Pauli operators

$$\begin{aligned} \sigma_1 &= \sigma_- + \sigma_+, \\ \sigma_2 &= i\,(\sigma_- - \sigma_+), \\ \sigma_3 &= \frac{1}{2i}\,[\sigma_1, \sigma_2] = |2\rangle\langle 2| - |1\rangle\langle 1| \end{aligned} \tag{2}$$

for the system. Here, $[A, B] = AB - BA$ denotes the commutator of A and B, and i is the imaginary unit. Clearly, $|1\rangle$ and $|2\rangle$ are also eigenstates of the inversion operator σ_3. This implies, that the system's time-invariant free Hamiltonian can be written in terms of σ_3 as

$$H_0 = E_1\,|1\rangle\langle 1| + E_2\,|2\rangle\langle 2| = \frac{\hbar\,\omega_R}{2}\,\sigma_3,$$

where $\hbar$ is the reduced Planck constant, $\omega_R = \hbar^{-1}\,(E_2 - E_1)$ denotes the system's resonance frequency and $E_1 = -E_2$ is assumed without loss of generality.

The system is driven by an external classical monochromatic electromagnetic field

$$u(t) = \varepsilon\,\hat{E}\cos(\omega_F\,t) \tag{3}$$

with unit polarisation vector ε, amplitude $\hat{E}$ and angular frequency ω_F (ref. Fig. 1, light blue snake arrow). This input explicitly does not depend on the state of the system, i.e. we do not consider feedback control here. The coupling between the system and the field is described by the dipole-interaction Hamiltonian

$$H_I(t) = -d\,u(t)\,(\sigma_+ + \sigma_-) = -d\,u(t)\,\sigma_1$$

with the transition dipole matrix element d assumed to be real and non-zero. It is common practice to express the coupling strength in terms of the Rabi frequency $\Omega = \frac{d\,\varepsilon\,\hat{E}}{\hbar}$, such that the total Hamiltonian of the system can be written as

$$H(t) = H_0 + H_I(t) = \hbar\left(\frac{\omega_R}{2}\sigma_3 - \Omega\cos(\omega_F\,t)\,\sigma_1\right). \tag{4}$$

Note, that within the scope of this paper, the widespread *rotating wave approximation* is not being made.

The Hamiltonian (4) is the generator of the unitary time evolution of the system according to the Schrödinger-von-Neumann equation. However, introducing damping phenomenologically as decoherence, induces non-unitary dynamics and thus, the system's time evolution is given by the Born-Markov master equation in Lindblad form [22], [23]

$$\dot{\rho} = -\frac{i}{\hbar}\,[H, \rho] + \Gamma\,\mathscr{D}[\sigma_-]\,\rho,\ \rho(0) = \rho_0, \tag{5}$$

where the pure or mixed state of the system at time t is represented by the positive semi-definite Hermitian density operator $\rho(t)$, $\mathrm{Tr}\{\rho\} = \mathrm{Trace}\{\rho\} = 1$, acting on the Hilbert space $\mathbb{C}^2$ of the system. The Lindblad superoperator

$$\mathscr{D}[c]\,\rho = c\,\rho\,c^\dagger - \frac{1}{2}\left(c^\dagger\,c\,\rho + \rho\,c^\dagger\,c\right), \tag{6}$$

defined for some arbitrary operator c, can be regarded as an irreversible loss channel, describing here the decay from level $|2\rangle$ to $|1\rangle$ mediated by the lowering operator σ_-.

A. Continuous measurement process

The measurement process constitutes a key difference between classical and quantum mechanical systems, as in the latter, it directly and inevitably influences the system's state. In fact, the so called backaction of a measurement adds a stochastic term to the deterministic system dynamics [7]. In the following, we consider a continuous measurement of the observable $\mathscr{O} = \frac{\sigma_3}{2}$ by weakly coupling the system to a readout probe field. This results in the measurement output [24], [25]

$$I(t) = \sqrt{\eta\,M}\,\mathrm{Tr}\left\{\left(\mathscr{O} + \mathscr{O}^\dagger\right)\rho(t)\right\} + \xi(t), \tag{7}$$

where $\eta \in [0, 1]$ denotes the detector efficiency ($\eta = 1$ implying perfect detection), $M > 0$ the interaction strength and $\xi(t)$ represents Gaussian white noise. The evolution of the system conditioned on the observation record (7) is then given by the stochastic master equation [12], [26]

$$\begin{aligned} \mathrm{d}\rho(t) = &-\frac{i}{\hbar}\,[H(t), \rho(t)]\,\mathrm{d}t + \Gamma\,\mathscr{D}[\sigma_-]\,\rho(t)\,\mathrm{d}t \\ &+ M\,\mathscr{D}[\mathscr{O}]\,\rho(t) + \sqrt{\eta\,M}\,\mathscr{H}[\mathscr{O}]\,\rho(t)\,\mathrm{d}W(t), \end{aligned} \tag{8}$$

where $\mathrm{d}W(t) = \xi(t)\,\mathrm{d}t$ is an infinitesimal Wiener increment satisfying $\mathbb{E}[\mathrm{d}W(t)] = 0, \mathbb{E}\left[\mathrm{d}W(t)^2\right] = \mathrm{d}t$. Here, the incremental notation highlights that (8) is a stochastic differential equation in Itô-form, where the superoperator

$$\mathscr{H}[c]\,\rho = c\,\rho + \rho\,c^\dagger - \mathrm{Tr}\left\{c\,\rho + \rho\,c^\dagger\right\}\rho, \tag{9}$$

defined for some arbitrary operator c, is the diffusion introduced by the measurement backaction and the second Lindblad term models the unconditional interaction with the measuring device [27].

Note, that while the stochastic master equation as stated in (8) describes a general continuous quantum measurement, it is most often used in the case of homodyne detection [21], [28].

B. Transformation to state space representation

The conditional dynamics of the continuously monitored two-level system are completely described by the stochastic master equation (8). In the following, an equivalent state space representation, conventionally used in control engineering, is derived.

Since the Pauli operators (2) and the identity operator $\mathbb{1}$ together form a basis of the vector space of Hermitian operators acting on $\mathbb{C}^2$, using the spinor representation

$$|1\rangle = \begin{bmatrix} 1 \\ 0 \end{bmatrix}, |2\rangle = \begin{bmatrix} 0 \\ 1 \end{bmatrix}, \tag{10}$$

the density operator can be expanded as linear combination

$$\begin{aligned}\rho(t) &= \frac{1}{2}\left(\mathbb{1} + x_1(t)\,\sigma_1 + x_2(t)\,\sigma_2 + x_3(t)\,\sigma_3\right) \\ &= \frac{1}{2}\begin{bmatrix} 1 - x_3(t) & x_1(t) + i x_2(t) \\ x_1(t) - i x_2(t) & 1 + x_3(t) \end{bmatrix},\end{aligned} \tag{11}$$

where the time-dependant dimensionless coefficients $x_j(t) \in \mathbb{R}, \sum x_j^2 \leq 1$, $j = 1,2,3$ are called Bloch coordinates. These constitute the state vector $x \in \mathbb{R}^3$. Most notably, $x_3 \in [-1,+1]$ gives the probability of the system to be in state $|1\rangle$ or $|2\rangle$, respectively, while $x_{1,2}$ describe the complex coherence. Taking the time derivative and substituting (8) yields the stochastic system dynamics in Itô state space form

$$\begin{aligned}\mathrm{d}x = &\underbrace{\begin{bmatrix} -\frac{\Gamma+M}{2}x_1 - \omega_R x_2 \\ \omega_R x_1 - \frac{\Gamma+M}{2}x_2 + 2\,\Omega\cos(\omega_F t)\,x_3 \\ -\Gamma\,(1+x_3) - 2\,\Omega\cos(\omega_F t)\,x_2 \end{bmatrix}}_{=:f(t,x)}\mathrm{d}t \\ &+ \underbrace{\sqrt{\eta M}\begin{bmatrix} -x_1 x_3 \\ -x_2 x_3 \\ 1 - x_3^2 \end{bmatrix}}_{=:g(x)}\mathrm{d}W \\ =&f(t,x)\,\mathrm{d}t + g(x)\,\mathrm{d}W, x(0) = x_0 \in \mathbb{R}^3.\end{aligned} \tag{12}$$

The output equation (7) is rewritten accordingly as

$$y = \underbrace{\sqrt{\eta M}\,x_3}_{=:h(x)} + \xi = h(x) + \xi, y \in \mathbb{R}. \tag{13}$$

Finally, on the interval $t \in [0,T]$, $T > 0$, the Euler-Maruyama method yields the discrete approximation

$$x_{k+1} = x_k + f(k\Delta t, x_k)\,\Delta t + g(x_k)\,\Delta W_k, \tag{14}$$

$$y_k = h(x_k) + \frac{\Delta W_k}{\Delta t}, \tag{15}$$

$$k = 0, \ldots, \frac{T}{\Delta t} - 1, \tag{16}$$

with step size Δt and $\Delta W_k \sim \mathscr{N}(0, \Delta t)$. In this form, a unique quantum mechanical feature of the system is easily seen, i.e. the fact, that the same stochastic term ΔW_k affects the state dynamics (14) as well as the measurement output (15), therefore effectively coupling both equations. This conditioning marks a substantial difference from classical stochastic differential equations.

III. OBSERVER DESIGN

Having derived a suitable stochastic state space representation for the two-level system, subsequently, a state observer is designed. Essentially, an observer is a separate dynamic system that reconstructs the internal states of a given reference system from its known input and measured output signals. The prerequisite for this is, that the system is *observable*. For system (12–13), this is established through the following lemma.

Lemma 1 ([29]): A non-linear system

$$\begin{aligned}\dot{x} &= f(t,x), x(0) = x_0 \in \mathbb{R}^n \\ y &= h(x), y \in \mathbb{R}\end{aligned}$$

is locally observable, if the observability matrix

$$Q(x) = \frac{\partial}{\partial x}\begin{bmatrix} L_f^0 h(x) & L_f h(x) & \ldots & L_f^{n-1} h(x) \end{bmatrix}^\top$$

with $L_f h(x) = \frac{\partial h}{\partial t} f(t,x)$ satisfies $\operatorname{rank} Q(x) = n$.

Since this condition is satisfied for $t \neq \frac{\pi(2n+1)}{2\,\omega_F}$, $n \in \mathbb{N}$, it is possible to reconstruct the full state vector x, and thus the entire density matrix ρ, from the recorded measurement data (7). This is accomplished by an extended Kalman filter [30].

As optimal state estimator, the Kalman filter is widely used in control engineering, especially in robotics and navigation. It arises from the minimisation of model uncertainties and measurement errors, and is evaluated recursively at each time step k. Conventionally, the filtering algorithm is split into two separate phases:

First, in the prediction phase, the current estimate of the state $\hat{x}_k^+$ is propagated through the deterministic system dynamics

$$\begin{aligned}\hat{x}_{k+1}^- &= \hat{x}_k^+ + f\left(k\Delta t, \hat{x}_k^+\right)\Delta t, \\ P_{k+1}^- &= A_k P_k^+ A_k^\top + Q\end{aligned} \tag{17}$$

to produce an *a priori* state estimate $\hat{x}_{k+1}^-$ for the next time step. Similarly, an *a priori* estimate of the prediction error covariance matrix P_{k+1}^- is computed. The initial guess $P_0^+ \geq 0$

encodes the confidence in the estimate of the initial condition $\hat{x}_0^+$. The state transition matrix

$$A_k = \mathbb{1} + \Delta t \left.\frac{\partial f}{\partial x}\right|_{k\Delta t, \hat{x}_k^+}$$

is the result of a local first order Taylor linearisation of the non-linear deterministic system dynamics and $Q \geq 0$ is the covariance matrix of the process noise induced by ΔW_k.

Secondly, in the correction phase, the latest measurement result y_k is incorporated by updating the predictions (17) to the *a posteriori* estimates

$$\begin{aligned} \hat{x}_{k+1}^+ &= \hat{x}_{k+1}^- + K_k \left(y_k - h\left(\hat{x}_k^+\right) \right), \\ P_{k+1}^+ &= \left(\mathbb{1} - K_k C_k \right) P_{k+1}^-. \end{aligned} \tag{18}$$

The observation matrix

$$C_k = \left.\frac{\partial h}{\partial x}\right|_{\hat{x}_{k+1}^-}$$

is the result of a local Taylor linearisation of the deterministic output function $h(x)$, while the Kalman gain

$$K_k = P_{k+1}^- C_k^\top \left(C_k P_{k+1}^- C_k^\top + R \right)^{-1} \tag{19}$$

additionally takes the covariance $R > 0$ of the measurement noise $(\Delta t)^{-1}\Delta W_k$ into consideration.

While linearising at every time step does limit the observer's theoretically guaranteed optimality, it constitutes a reasonable payoff between near-optimality and computational cost.

IV. RESULTS

In this section, several numeric simulations are carried out to validate and showcase the performance of the Kalman filtering scheme. The employed system parameters are listed in Tab. I below. As common in quantum mechanics, the

TABLE I

PARAMETER VALUES USED FOR THE SIMULATIONS.

parameter	symbol	value
decay rate	Γ	$10\,\mathrm{s}^{-1}$
resonance frequency	ω_R	5Γ
Rabi frequency	Ω	3Γ
irradiation frequency	ω_F	4Γ
interaction strength	M	$1\,\mathrm{s}^{-1}$
detection efficiency	η	80 %

parameters here are expressed in terms of the decay rate Γ, while the time t will be in units of Γ^{-1}. Note, that the values are chosen arbitrarily and are not based on an actual physical system. Furthermore, without loss of generality, the system is initially prepared purely in the excited state

$$x_0 = \begin{bmatrix} 0 & 0 & 1 \end{bmatrix}^\top.$$

The time evolution of the driven and damped two-level system resulting from this setup is visualised in Fig. 2. Here, the dimensionless Bloch states $x_j(t)$, $j = 1,2,3$ are interpreted

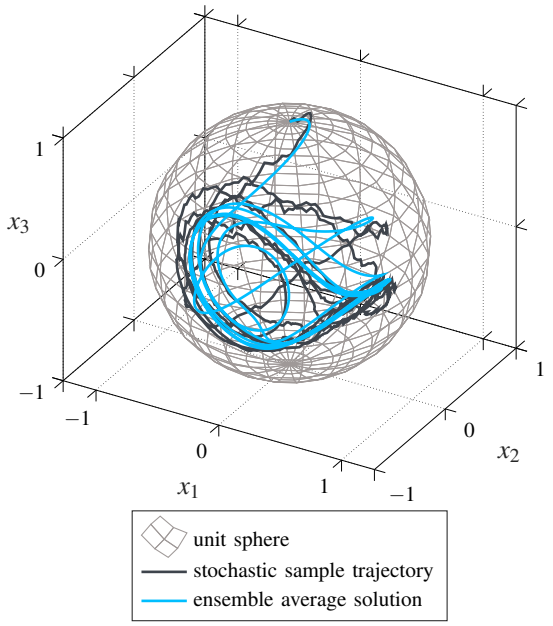

Fig. 2. Visualisation of the time evolution of the continuously measured driven and damped two-level system (14), Tab. I in Euclidean space.

as Euclidean coordinates. Since $\sum x_j^2 \leq 1$, the trajectories are confined to a unit sphere, where pure states lie on the surface and mixed states inside [31]. One possible realisation of the stochastic system evolution (14) is depicted in black, while the deterministic ensemble average solution is shown in light blue. As can be seen, the diffusive measurement backaction $g(x)\,\mathrm{d}W$ has a non-negligible stochastic influence on the trajectory. Due to the Lindbladian damping terms, the system converges to a periodic stationary oscillation, while the continuous excitation (3) prevents the system from reaching a steady state. The corresponding measurement output is plotted in Fig. 3. Clearly, due to the division by

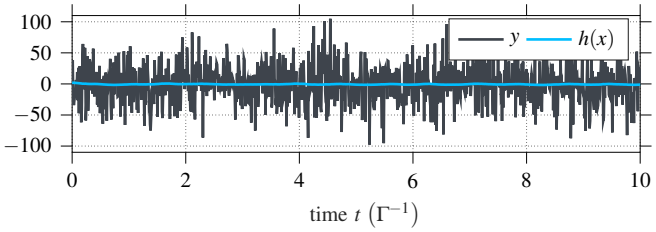

Fig. 3. Measurement record (15) corresponding to the stochastic trajectory shown in Fig. 2.

Δt in (15), the stochastic term affecting the measurement signal has a significantly higher variance than the state diffusion. Nonetheless, the Kalman filter is able to exploit these measurements, as shown in the following.

The employed Kalman filter is set up with the experimentally tuned covariance matrices

$$\begin{aligned} P_0^+ &= \mathrm{diag}\left(\begin{bmatrix} 1 & 1 & 1 \end{bmatrix} \right), \\ Q &= \mathrm{diag}\left(\Delta t \begin{bmatrix} 1 & 1 & \frac{1}{10} \end{bmatrix} \right), \\ R &= \frac{1}{\sqrt{\Delta t}}, \end{aligned}$$

for the initial condition guess, the process noise and the measurement noise, respectively, and initially assumes a totally mixed state with equal probabilities

$$\hat{x}_0^+ = \begin{bmatrix} 0 & 0 & 0 \end{bmatrix}^\top.$$

The simulation results of the state estimation are presented in Fig. 4. The three subplots show both the evolution of the

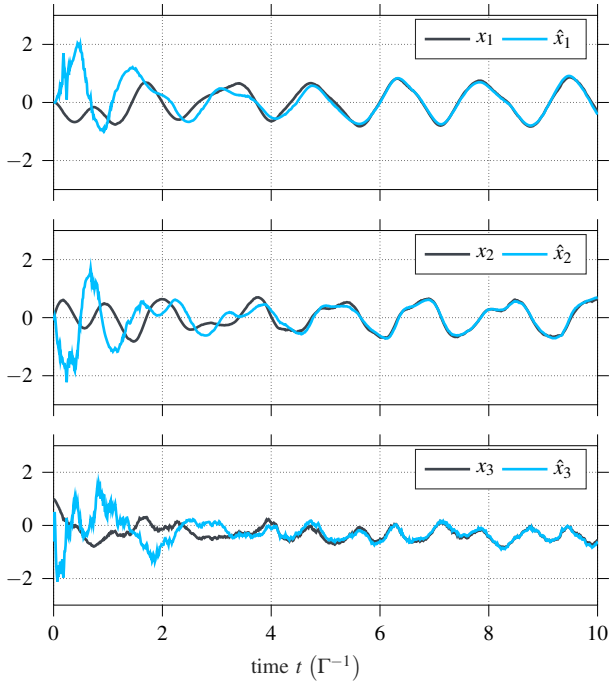

Fig. 4. System (14) and observer (17–19) state evolution.

true state $x(t)$ in black and the evolution of the observer state $\hat{x}(t)$ in light blue. As can be seen, it takes the Kalman filter roughly 4 to $5\Gamma^{-1}$ to correct the initial estimation error and to accurately reproduce the true system states. This is achieved by rather aggressive corrections (18) in the beginning, while after convergence, the *a priori* estimates are updated much less. This is shown in Fig. 5. It turns

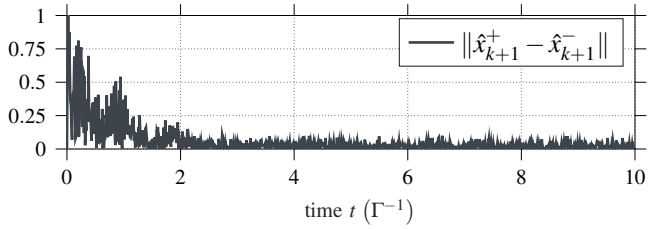

Fig. 5. Norm of the conditioning on the latest measurement result done by the Kalman filter corrector.

out, that despite the high variance measurement noise, the Kalman filter does not simply propagate the deterministic drift dynamics of the system, but actually conditions quite heavily on the latest measurement result in order to improve the estimation accuracy.

In order to quantitatively assess the observer performance, the fidelity [32]

$$F(\rho, \hat{\rho}) = \mathrm{Tr}\left\{ \sqrt{\sqrt{\rho}\,\hat{\rho}\,\sqrt{\rho}} \right\}^2, F \in [0, 1], \qquad (20)$$

which provides a distance measure between two quantum states ($F = 1$ implying equality), is computed for the reconstructed density operator ρ and its observed counterpart $\hat{\rho}$. This is plotted in Fig. 6 over time. Clearly, the fidelity

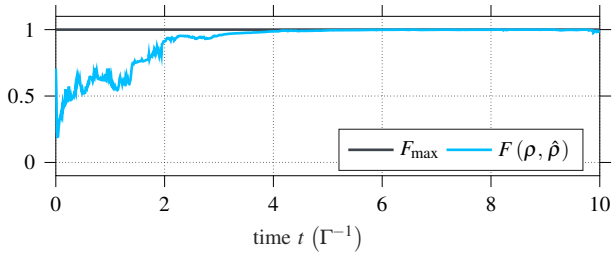

Fig. 6. Fidelity between the reconstructed density operator ρ and its estimate $\hat{\rho}$.

asymptotically converges to its upper bound $F_{\max} = 1$, implying the Kalman filter successfully reconstructs the full density operator ρ from the measurement data (15) using the underlying system model (14).

A. Parameter estimation

In the following, the Kalman filter (17–19) is modified to not only estimate the density operator, but also key system parameters, i.e. the resonance frequency ω_R and the decay rate Γ. In control engineering, it is common for these parameters to be introduced as additional time-constant system states $x_4 = \omega_R, x_5 = \Gamma, \dot{x}_{4,5} = 0$, such that observing the augmented state vector automatically provides an estimate for these parameters as well. The theoretical feasibility of this approach is again shown through Lemma 1, whose observability condition is also satisfied by the extended system. The practical applicability is demonstrated in Fig. 7 and 8. Here,

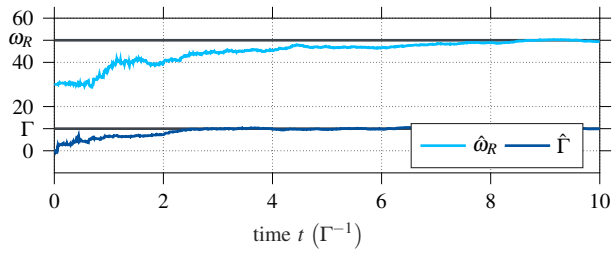

Fig. 7. Evolution of the observer parameter states corresponding to the resonance frequency ω_R and the decay rate Γ.

the same simulation as before has been carried out, however, incorrect initial values $\hat{x}_4^+(0) = 25, \hat{x}_5^+(0) = 0$ were assumed for the parameter states of the observer. Fig. 7 shows the time evolution of the observed resonance frequency in light blue and the decay rate in dark blue, respectively. As can be seen, both asymptotically converge against their actual value. Contemporaneously, the regular system states are estimated, the corresponding fidelity is plotted in Fig. 8.

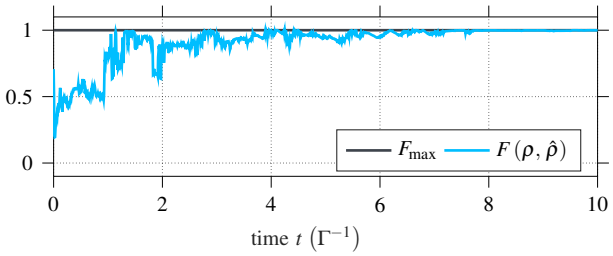

Fig. 8. Fidelity between the reconstructed density operator ρ and its estimate $\hat{\rho}$, when observing additionally the resonance frequency ω_R and the decay rate Γ.

Naturally, the Kalman filter takes more time than before to precisely replicate the evolution of the true density operator, but ultimately, it does prove successful. In conclusion, the observer does not only provide an accurate online estimate of the system's resonance frequency ω_R and its decay rate Γ, but also reconstructs the full quantum state ρ of the system.

V. Conclusion

In this paper, an engineering approach to a quantum control problem has been studied. Using an extended Kalman filter, we were able to dynamically estimate the full state and identify multiple parameters of an open two-level quantum system. Thereby, the observer showed fast convergence and achieved high fidelities.

Overall, the conditioning of the system dynamics on the measurement results in quantum mechanics poses an intriguing premise for future research. Hence, expanding on the groundwork established here, we aim to explore different feedback control strategies and analyse a wider range of systems.

ACKNOWLEDGMENT

This work was conducted in the framework of the Graduate School 2642/1 "Towards Graduate Experts in Photonic Quantum Technologies" (project ID 431314977) funded by the German Research Foundation (DFG – Deutsche Forschungsgemeinschaft).

References

[1] Hideo Mabuchi and Navin Khaneja. Principles and applications of control in quantum systems. *International Journal of Robust and Nonlinear Control*, 15(15):647–667, 2005.

[2] Constantin Brif, Raj Chakrabarti, and Herschel Rabitz. Control of quantum phenomena: past, present and future. *New Journal of Physics*, 12(7):075008, 2010.

[3] Mazyar Mirrahimi, Pierre Rouchon, and Gabriel Turinici. Lyapunov control of bilinear Schrödinger equations. *Automatica*, 41(11):1987–1994, 2005.

[4] Sen Kuang and Shuang Cong. Lyapunov control methods of closed quantum systems. *Automatica*, 44(1):98–108, 2008.

[5] Sen Kuang and Shuang Cong. Population Control of Equilibrium States of Quantum Systems via Lyapunov Method. *Acta Automatica Sinica*, 36(9):1257–1263, 2010.

[6] Shuang Cong and Fangfang Meng. A survey of quantum Lyapunov control methods. *TheScientificWorldJournal*, 2013:967529, 2013.

[7] Ju-Ju Hu, Qiang Ke, and Ying-Hua Ji. Perfect Manipulation of Open Stochastic Quantum Systems with Imperfect Detection. *International Journal of Control, Automation and Systems*, 20(3):831–841, 2022.

[8] K. Kashima and N. Yamamoto. Control of Quantum Systems Despite Feedback Delay. *IEEE Transactions on Automatic Control*, 54(4):876–881, 2009.

[9] H. Mabuchi. Dynamical identification of open quantum systems. *Quantum and Semiclassical Optics: Journal of the European Optical Society Part B*, 8(6):1103–1108, 1996.

[10] Jay Gambetta and H. M. Wiseman. State and dynamical parameter estimation for open quantum systems. *Physical Review A*, 64(4), 2001.

[11] P. Warszawski, Jay Gambetta, and H. M. Wiseman. Dynamical parameter estimation using realistic photodetection. *Physical Review A*, 69(4), 2004.

[12] Zhengui Xue, Hai Lin, and Tong Heng Lee. Identification and control of a two-level open quantum system. In *IEEE Conference on Decision and Control and European Control Conference*, pages 6254–6259. IEEE, 2011.

[13] Shuang Cong, Yaru Tang, Sajede Harraz, Kezhi Li, and Jingbei Yang. On-line quantum state estimation using continuous weak measurement and compressed sensing. *Science China Information Sciences*, 64(8), 2021.

[14] Shuang Cong, Yaru Tang, and Kezhi Li. State Transfer of Two-level Quantum System Feedback Control Based on Online State Estimation. In *2021 40th Chinese Control Conference (CCC)*, pages 6301–6306. IEEE, 2021.

[15] Andrew Silberfarb, Poul S. Jessen, and Ivan H. Deutsch. Quantum state reconstruction via continuous measurement. *Physical review letters*, 95(3):030402, 2005.

[16] Greg A. Smith, Andrew Silberfarb, Ivan H. Deutsch, and Poul S. Jessen. Efficient quantum-state estimation by continuous weak measurement and dynamical control. *Physical review letters*, 97(18):180403, 2006.

[17] Weichao Liang, Nina H. Amini, and Paolo Mason. On estimation and feedback control of spin-1/2 systems with unknown initial states. *IFAC-PapersOnLine*, 53(2):5863–5868, 2020.

[18] A. C. Doherty, S. M. Tan, A. S. Parkins, and D. F. Walls. State determination in continuous measurement. *Physical Review A*, 60(3):2380–2392, 1999.

[19] A. C. Doherty and K. Jacobs. Feedback control of quantum systems using continuous state estimation. *Physical Review A*, 60(4):2700–2711, 1999.

[20] J. M. Geremia, John K. Stockton, Andrew C. Doherty, and Hideo Mabuchi. Quantum Kalman filtering and the Heisenberg limit in atomic magnetometry. *Physical review letters*, 91(25):250801, 2003.

[21] John K. Stockton, J. M. Geremia, Andrew C. Doherty, and Hideo Mabuchi. Robust quantum parameter estimation: Coherent magnetometry with feedback. *Physical Review A*, 69(3), 2004.

[22] Wiseman, Howard M. and Milburn, Gerard J. *Quantum Measurement and Control*. Cambridge University Press, Cambridge, online-ausg edition, 2009.

[23] C. Altafini and F. Ticozzi. Modeling and Control of Quantum Systems: An Introduction. *IEEE Transactions on Automatic Control*, 57(8):1898–1917, 2012.

[24] Mazyar Mirrahimi and Ramon van Handel. Stabilizing Feedback Controls for Quantum Systems. *SIAM Journal on Control and Optimization*, 46(2):445–467, 2007.

[25] Wiseman. Quantum theory of continuous feedback. *Physical Review A*, 49(3):2133–2150, 1994.

[26] Shahid Qamar, Shuang Cong, and Bilal Riaz. Lyapunov-based feedback control of two-level stochastic open quantum systems. In *2017 IEEE International Conference on Cybernetics and Intelligent Systems (CIS) and IEEE Conference on Robotics, Automation and Mechatronics (RAM)*, pages 48–53. IEEE, 2017.

[27] Andrew C. Doherty, Salman Habib, Kurt Jacobs, Hideo Mabuchi, and Sze M. Tan. Quantum feedback control and classical control theory. *Physical Review A*, 62(1), 2000.

[28] Andrew Silberfarb and Ivan H. Deutsch. Continuous measurement with traveling-wave probes. *Physical Review A*, 68(1), 2003.

[29] Alberto Isidori. *Nonlinear control systems*. Communications and control engineering series. Springer, London, 3. ed. edition, 1995.

[30] Dan Simon. *Optimal state estimation: Kalman, H [infinity] and nonlinear approaches*. Wiley-Interscience, Hoboken, N.J, 2006.

[31] Domenico D'Alessandro. *Introduction to Quantum Control and Dynamics*. Chapman and Hall/CRC Applied Mathematics and Nonlinear Science Ser. CRC Press LLC, London, 1st ed. edition, 2008.

[32] Richard Jozsa. Fidelity for Mixed Quantum States. *Journal of Modern Optics*, 41(12):2315–2323, 1994.